Crystal chemistry of ivanyukite group minerals, A3-xH1+x[Ti4O4(SiO4)3] (H2O)n (A=Na,K,Cu), (n=6-9, x=0-2): crystal structures, ion-exchange, chemical evolution

7 authors, including:

Taras L Panikorovskii
Kola Science Centre
144 PUBLICATIONS   **864** CITATIONS

SEE PROFILE

Nataliia Ianicheva
12 PUBLICATIONS   **121** CITATIONS

SEE PROFILE

Ya. A. Pakhomovsky
Kola Science Centre
115 PUBLICATIONS   **1,196** CITATIONS

SEE PROFILE

Vladimir V. Shilovskikh
Saint Petersburg State University
160 PUBLICATIONS   **993** CITATIONS

SEE PROFILE

Crystal chemistry of ivanyukite group minerals, A_{3-x}H$_{1+x}$[Ti$_4$O$_4$(SiO$_4$)$_3$](H$_2$O)$_n$ (A = Na, K, Cu), (n = 6-9, x = 0-2): crystal structures, ion-exchange, chemical evolution

Taras L. Panikorovskii[1,2]*, Victor N. Yakovenchuk[1], Nataliya Yu. Yanicheva[1], Yakov A. Pakhomovsky[1], Vladimir V. Shilovskikh[3], Vladimir N. Bocharov[3] and Sergey V. Krivovichev[1,2]

[1] *Kola Science Centre, Russian Academy of Sciences, 14 Fersman Street, Apatity 184200, Russia*

[2] *Department of Crystallography, St. Petersburg State University, 7–9 University Emb, St. Petersburg 199034, Russia*

[3] *Geo Environmental Centre "Geomodel", St. Petersburg State University, Ul'yanovskaya Str., St. Petersburg 198504, Russia*

* Corresponding author. E-mail: t.panikorovskii@ksc.ru

Mineralogical Society

Abstract

Microporous titanoslicates with the pharmacosiderite structure and the general formula $A_{3-x}H_{1+x}[Ti_4O_4(SiO_4)_3](H_2O)_n$ (A = Na, K, Cu), (n = 6-9, x = 0-2) are outstanding in their ion-exchange properties. The ivanyukite mineral group consists of three species, one of which has two polymorphs. The minerals forming a progressive series "ivanyukite-Na-T → ivanyukite-Na-C → ivanyukite-K → Cu-rich ivanyukite-K → ivanyukite-Cu" have been studied by single-crystal X-ray diffraction, electron microprobe analysis and Raman spectroscopy. The microporous heteropolyhedral framework of the ivanyukite-group minerals is based upon cubane-like $[Ti_4O_4]^{8+}$ clusters that share common corners with SiO_4 tetrahedra to form wide three-dimensional channels suitable for the migration of Na^+, K^+ and Cu^{2+} ions. Ivanyukite-Na-T that has a $R3m$ symmetry loses Na^+ in aqueous solutions *via* the substitution $Na^+ + O^{2-} \leftrightarrow \square + OH^-$, which allows for the migration of K^+ ions and transformation of initial structure into the cubic ($P\overline{4}3m$) ivanyukite-Na-C polymorph or into ivanyukite-K, when most of Na is lost. Natural ivanyukite-Na-C is shown to contain domains of both $R3m$ (subordinate) and $P\overline{4}3m$ (dominant) symmetry with the chemical composition determining the stability and dominance of cubic or trigonal forms. Incorporation of Cu into the crystal structure ivanyukite-K via the substitution $K^+ + OH^- \leftrightarrow Cu^{2+} + O^{2-}$ in aqueous solutions results in the formation of ivanyukite-Cu. Post-crystallisation processes (such as exchange of Na^+, K^+, Cu^{2+}, and/or hydration/dehydration of primary phases) are widespread in hyperagpaitic rocks of the Kola alkaline massif and the respective mineral transformations contribute to the diversity of mineral species.

Keywords

Ivanyukite-Na-*T*, ivanyukite-Na-*C*, ivanyukite-K, ivanyukite-Cu, pharmacosiderite, ion-exchange, alkaline massif, Khibiny, Arctic.

Introduction

Microporous titanosilicates (*MT*s) constitute an important class of molecular sieves whose frameworks are composed from $[SiO_4]$ tetrahedra and $[TiO_6]$ octahedra (Anderson *et al.*, 1995; Clearfield, 2001). Currently more than 100 mineral species can be considered as *MT*s, which crystallize in 30 different framework types (Chukanov and Pekov, 2005). In many cases, their synthetic analogues were synthesized after their mineralogical discoveries and found extensive applications in catalysis, adsorption, separation and ion-exchange (Rocha and Anderson, 2000; Milne *et al.*, 2006; Anson *et al.*, 2009; Lin *et al.*, 2012; Popa and Pavel, 2012). The most studied mineral analogues in material science are the synthetic counterparts of zorite (Engelhard titanium silicate, ETS-4), ivanyukite (Grace titanium silicate, GTS, synthetic ivanyukite, SIV), kamenevite (Aveiro and Manchester, AM-2, Surfactant-templated silica, STS) and sitinakite (ion sieve, IONSIV-911, Texas A and M,TAM-5, Surfactant-templated silica, STS, crystalline titanosilicate material, CST) (Oleksiienko *et al.*, 2017). All the mineral species that served as prototypes of synthetic materials were first discovered in the Khibiny or Lovozero alkaline massifs of Kola Peninsula, Russia. Less known and less studied in chemistry are minerals of the lovozerite group (tisinalite), hilairite group (pyatenkoite-(Y)), and labuntsovite group that also have pronounced ion-exchange and photocatalytic properties (Chukanov and Pekov, 2005; Gerasimova *et al.*, 2019).

The *MT* materials based upon the pharmacosiderite framework topology (Behrens *et al.*, 1998a) possess outstanding ion-exchange properties (Majzlan *et al.*, 2019). Chapman & Roe (1990) first synthesized the analogue of ivanyukite-K and reported on the formation of its H- and

Cs- exchanged phases. Later studies provided data on preparation, crystal structures and ion-exchange properties of the $A_3H[Ti_4O_4(XO_4)_3](H_2O)_n$ compounds, where A = H, Na, K, Rb, Cs; X = Si, Ge (Behrens *et al.*, 1996, 1998b; Behrens and Clearfield, 1997; Dadachov and Harrison, 1997). These compounds have been considered as prospective materials for the selective removal of Cs and Sr from radioactive waste aqueous solutions. Calcination of Cs- and Sr-exchanged synthetic ivanyukite up to 1000 °C results in the formation of stable titanate ceramics akin to synthetic rock (synroc) composed of rutile, tuasonite, pyrochlore, hollanite and 'leucite' (Britvin *et al.*, 2016).

There are three ivanyukite-group minerals currently approved by the IMA CNMNC: (ivanyukite-Na (IMA-2007-041), ivanyukite-K (IMA-2007-042) and ivanyukite-Cu (2007-043). In nature, three ivanyukite-group minerals occur in natrolitized microcline-aegirine-sodalite veins within an orthoclase-bearing urtite of the Koashva apatite mine (Fig. 1), Khibiny alkaline massif, Kola Peninsula, Russia (Yakovenchuk *et al.*, 2009). They are found in a hyperagpaitic low-temperature hydrothermal assemblage in association with natrolite, villiaumite, sitinakite, djerfisherite, sazykinaite-(Y), lucasite-(Ce), and amorphous bitumens. According to Yakovenchuk *et al.* (2011), all ivanyukite-group minerals crystallize during later stages of hydrothermal activity. In the original study by Yakovenchuk *et al.* (2009), the crystal structure was reported for ivanyukite-Na-*T* only.

Herein we report the results of crystal-structure refinements of ivanyukite-Na-*C*,-Na-*T*, -K and Cu-rich ivanyukite-K obtained during the course of ion-exchange experiments. The new finds of ivanyukite-Na and ivanyukite-K, from the Oleniy Ruchey and Koashva mines allowed the acquisition of more chemical and structural data. The new samples have been deposited at the Museum and Exhibition Center (MEC) in Kirovsk, Murmansk region, Russia under catalogue no MEC-3184 (ivanyukite-Na-*T*), MEC-3183 (ivanyukite-Na-*C*), MEC-517 (ivanyukite-K). The results of the current study provide an important insight into the transformational nature of the ivanyukite-group minerals.

Samples and experimental

Four samples of ivanyukite-group minerals were extracted from the aegirine-microcline-natrolite vein of the Koashva apatite mine, Khibiny, Kola peninsula, Russia (Fig. 2). In all samples, ivanyukite-group minerals form blocky crystals up to 1 mm in size, which grow on the surface of natrolite or form inclusions in it. Ivanyukite-group minerals are closely associated with pectolite, vinogradovite, sazykinaite-(Y), djerfisherite and chlorbartonite. Ivanyukite-Na-*T* forms epitaxial colorless crusts up to 100 μm thick on the surfaces of pseudo-cubic crystals of sitinakite (Fig. 2c) or are present as individual colorless rhombohedral crystals. Ivanyukite-Na-*C* forms blocky pale-orange (Fig. 2a) or milky-pink cubic crystals growing on natrolite. Ivanyukite-K occurs as pale-blue crystals associated with chlorbartonite (Fig. 2b), whereas ivanyukite-Cu was found as emerald green or light green cubic crystals in a cavity within partially decomposed djerfisherite (Fig. 2d). The amount of natural material of ivanyukite-K and ivanyukite-Cu in natural samples was rather small and their analogues were prepared by ion-exchange reactions using crystals of ivanyukite-Na-*T*.

For the structural studies, the colorless crusts of ivanyukite-Na-*T* and blocky pale-orange crystals of ivanyukite-Na-*C* were selected. In order to prepare an analogue of ivanyukite-K, the crystals of ivanyukite-Na-*T* used in the structural study were kept in water for 1 hour. Throughout this process, the crystals have not changed their colour. The Cu-rich ivanyukite-K was prepared by placing crystals of ivanyukite-Na-*T* into 1M solution of $CuCl_2$ for 96 hours under ambient conditions. The resulting crystals had a distinctly green colour.

The chemical composition of the studied samples was determined by wavelength-dispersive spectrometry on a Cameca MS-46 electron microprobe (Geological Institute, Kola Science Centre, Russian Academy of Sciences, Apatity) operating at 20 kV, 20-30 nA, with a 20 μm beam diameter. The following standards were used: lorenzenite (Na, Ti), pyrope (Al), wollastonite (Si, Ca), wadeite (K), synthetic $MnCO_3$ (Mn), hematite (Fe), metallic copper (Cu)

and synthetic $LiNbO_3$ (Nb). Analyses were performed with the probe defocused up to 20 μm, and by continuous movement (up to 100 μm from start point) of the sample to minimize mineral damage and the loss of Na and H_2O during the 10s counting time. Compositions of exchanged forms were investigated with a Hitachi S-3400N scanning electron microscope (Geomodel Resource Center, St. Petersburg State University) equipped with an INCA 500 WDS detector operating at 20–30 nA and 20 kV. The analyses were performed with a beam size of 5-20 μm and with a counting time of 10–20/10 s on peaks/background, respectively, for each chemical element. The following standards were used: albite (Na, Al), benitoite (Ti), olivine (Fe), diopside (Si, Ca), orthoclase (K), rhodonite (Mn), metallic niobium (Nb) and copper (Cu). The presence of OH groups and molecular H_2O was confirmed by Raman spectroscopy. The H_2O content was calculated according to the crystal-structure data.

The Raman spectra were obtained from the surface of the crystals at room temperature using a wavelength of 514 nm in the range from 4000 to 80 cm^{-1} using a Horiba Jobin-Yvon LabRam HR 800 spectrometer, 8 mW laser power and counting time 60 s (Geomodel Resource Center, St. Petersburg State University). The baseline correction was carried out using the algorithms in the OriginPro 8.1 software package.

The crystal-structure studies were carried out at the X-ray Diffraction Resource Centre of St. Petersburg State University by means of the Oxford diffraction Xcalibur EOS and Supernova diffractometers equipped with CCD detectors using monochromatic Mo$K\alpha$ radiation (λ = 0.71069 Å) at room temperature. More than a quarter of the diffraction sphere was collected for the cubic crystals and more than half for the trigonal crystals (scanning step 1°, exposure time 10-100 s). The data were integrated and corrected by means of the CrysAlisPro program package, an empirical absorption correction using spherical harmonics was applied, as implemented in the SCALE3 ABSPACK scaling algorithm (Agilent Technologies, 2014). The crystal structures were refined using the SHELXL software package (Sheldrick, 2015). The crystal structures were drawn using the VESTA 3 program (Momma and Izumi, 2011).

Occupancies of the cation sites were calculated from the experimental site-scattering factors (except for the low-occupied sites) in accordance with the empirical chemical composition. The H sites could not be located.

The crystal structure of ivanyukite-Na-*T* was refined to $R_1 = 0.099$ ($R_{int} = 0.095$) for 1303 independent reflections with $F_o > 4\sigma(F_o)$ in *R*3*m* space group. The crystal structures of ivanyukite-Na-*C*, ivanyukite-K and Cu-rich ivanyukite-K were refined to $R_1 = 0.098$ ($R_{int} = 0.16$), $R_1 = 0.048$ ($R_{int} = 0.031$) and $R_1 = 0.047$ ($R_{int} = 0.035$) for 1954, 632 and 648 independent reflections, respectively, in $P\bar{4}3m$ space group. The data obtained for ivanyukite-Na-*C* were also integrated in the *R*3*m* space group ($R_1 = 0.098$, $R_{int} = 0.085$, 711 independent reflections), which, however, did not improve the refinement notably. Soft restraints were applied to thermal ellipsoids of extra-framework sites in the crystal structure of ivanyukite-Na-*T*. Atom labels are given according to Yakovenchuk *et al.* (2009).

Nomenclature

Ivanyukite group minerals belong to pharmacosiderite supergroup (Rumsey *et al.*, 2010). According to Yakovenchuk *et al.* (2009) the nomenclature of the ivanyukite-group minerals is based on the dominant extra-framework cation (Na, K, Cu) and the symmetry of the crystal structure. Ivanyukite-Na may crystallize in the cubic $P\bar{4}3m$ and trigonal *R*3*m* space groups with modifiers *T* = trigonal and *C* = cubic used to distinguish between two modifications (Nickel and Grice, 1998). The ordering of the extra-framework cations over two or more sites was not taken into account.

For microporous zeolite-group minerals disordered extra-framework cations with low occupancies are considered jointly. In this work we use a *dominant-valency rule* for the definition of ivanyukite-group minerals. The rule states that the dominant ion (vacancy) of the dominant valence state is considered for the nomenclature purposes (Hatert and Burke, 2008; Bosi *et al.*, 2019). For example, in the original description, the Cu^{2+} is dominant extra-

framework cation for ivanyukite-Cu ($Cu_{0.62}K_{0.43}Na_{0.04}Ca_{0.03}$). In our case ($K_{0.76}Cu_{0.45}Ca_{0.04}$) the dominant root charge is 1+ (61%) and the studied sample is Cu-rich ivanyukite-K.

The ivanyukite-group minerals manifest the zeolitic properties, leading to the variable H_2O content for different crystals of the same mineral depending on its extra-framework cation contents (Coombs *et al.*, 1998).

Chemical composition

Analytical results for the structurally characterized ivanyukite-group minerals are provided in Table 1 in comparison with the previously determined compositions of ivanyukite-K and ivanyukite-Cu (Yakovenchuk *et al.*, 2009). The empirical formulas of the ivanyukite-group minerals were calculated on the basis of Si = 3 (instead of Si+Al = 3 used by Yakovenchuk *et al.* (2009), since all analyses are deficient with respect to the octahedral cations). The following empirical formulas have been obtained:

$(Na_{1.83}K_{0.92}Ca_{0.03})_{\Sigma 2.78}[(Ti_{3.66}Nb_{0.18}Fe^{2+}_{0.03}Al_{0.01})_{\Sigma 3.88}\{O_{2.44}(OH)_{1.56}\}_{\Sigma 4.00}(SiO_4)_3 \cdot 5.50H_2O$ − ivanyukite-Na-*T*;

$(Na_{1.29}K_{0.97}Ca_{0.02})_{\Sigma 2.28}[(Ti_{3.58}Nb_{0.16}Fe^{2+}_{0.02}Al_{0.02}Mn_{0.01})_{\Sigma 3.79}\{(OH)_{2.46}O_{1.54}\}_{\Sigma 4.00}(SiO_4)_3 \cdot 5.80H_2O$ − ivanyukite-Na-*C*;

$(K_{1.07}Na_{0.12}Ca_{0.04})_{\Sigma 1.23}[(Ti_{3.63}Nb_{0.17}Fe^{2+}_{0.03}Al_{0.01}Mn_{0.01})_{\Sigma 3.85}\{(OH)_{3.25}O_{0.75}\}_{\Sigma 4.00}(SiO_4)_3 \cdot 4.00H_2O$ − ivanyukite-K (ion-exchanged from);

$(K_{0.76}Cu_{0.45}Ca_{0.04})_{\Sigma 1.25}[(Ti_{3.56}Nb_{0.17}Fe^{2+}_{0.03}Al_{0.01})_{\Sigma 3.77}\{(OH)_{3.08}O_{0.92}\}_{\Sigma 4.00}(SiO_4)_3 \cdot 3.76H_2O$ − Cu-rich ivanyukite-K (ion-exchanged from).

Raman spectroscopy

The Raman spectra of ivanyukite-Na-*T*, ivanyukite-Na-*C*, and Cu-rich ivanyukite-K are shown in Fig. 3. The spectrum of cubic Cu-rich ivanyukite-K is similar to that of pharmacosiderite from Cornwall, England, taken from sample R050574 of the RRUFF project (Lafuente *et al.*, 2015). The assignments of the absorption bands were made by analogy with structurally related pharmacosiderite (Frost and Kloprogge, 2003; Filippi, 2004; Filippi *et al.*, 2007) and titanosilicates (Celestian *et al.*, 2013; Pakhomovsky *et al.*, 2018; Yakovenchuk *et al.*, 2019) and are given in Table 2.

The intense vibrational bands at 961, 929, 924, and 1030 cm^{-1} can be attributed to asymmetric stretching vibrations of SiO_4 tetrahedra, while the bands at 840, 844, and 845, 941 cm^{-1} are assigned to symmetric vibration modes involving the same bonds (Filippi, 2004; Celestian *et al.*, 2013). Weak bands at 714 and 716 cm^{-1} observed for ivanyukite-Na-*C* and Cu-rich ivanyukite-K may be attributed to the hydroxyl deformation (librational) mode (Frost and Kloprogge, 2003; Seki *et al.*, 2020). The most intense bands at 595 and 599 cm^{-1} for rhombohedral and cubic ivanyukite-Na are significantly shifted (by ~ 60 cm^{-1}) in comparison with the band at 533 cm^{-1} observed in the spectrum of Cu-rich ivanyukite-K and are related to the asymmetric bending vibrations of Si–O bonds or overlapping stretching vibrations of Ti–O bonds (Filippi *et al.*, 2007; Celestian *et al.*, 2013). This band also can be due to Cu−O stretching vibrations of mixed Cu−O −Ti stretching vibrations involving a Cu−O3 bond. The bands in the range 350–500 cm^{-1} correspond to symmetric bending vibrations of O–Si–O bonds and overlapping stretching vibrations of Ti–O bonds (Filippi *et al.*, 2007; Pakhomovsky *et al.*, 2018; Yakovenchuk *et al.*, 2019). The bands at 460 and 494 cm^{-1} assigned to different modes of Ti–O stretching vibrations. Bands of different intensities in the region of 200–350 cm^{-1} belong to the different bending vibration modes of the Ti–O bonds in TiO_6 octahedra (Frost and Kloprogge, 2003; Filippi, 2004). The bands with the wave numbers below 200 cm^{-1} belong to translational vibrations. The band at 126-128 cm^{-1} is observed in the Raman spectra of Na-bearing samples

and is absent in the Raman spectrum of the Na-free Cu-rich ivanyukite-K and probably responds to translation modes of Na.

In the spectra, there are weak characteristic bands of the ν_2 bending vibrations of the H−O−H bonds in the range of $1600-1625$ cm^{-1}. The bands in the region of $3250–3400$ cm^{-1} (Figure 3) correspond to the stretching vibrations in the O−H bonds of hydroxyl groups, whereas bands in the range $3440–3450$ cm^{-1} correspond to the same vibrations in the H_2O molecules (Seki *et al.*, 2020).

In general, the spectrum of ivanyukite-Na-*C* is intermediate between the spectra of rhombohedral ivanyukite-Na-*T* and cubic Cu-rich ivanyukite-K. It contains bands near 128, 340, 370 and 590 cm^{-1} that are characteristic of ivanyukite-Na-*T* and at the same time has bands near 490 and 714 cm^{-1} that are characteristic of Cu-rich ivanyukite-K. This can be explained by the presence of domains with both trigonal and cubic symmetries within the same crystals of ivanyukite-Na-*C*.

Crystal structure

The crystal data, data collection and structure refinement details are given in Table 3, atom coordinates are in Tables 4-8. Anisotropic displacement parameters, selected bond lengths and other details of the structure refinement are deposited as a supplementary CIF (Crystallographic Information File).

The crystal structures of all ivanyukite-group minerals studied (Fig. 4) possess a pharmacosiderite structure topology and are based upon topologically identical three-dimensional frameworks (Krivovichev, 2005). The main structural feature of the group is the presence of cubane-like $[Ti_4O_4]^{8+}$ clusters formed by four edge-sharing TiO_6 octahedra (Oleksiienko *et al.*, 2017). The $[Ti_4O_4]^{8+}$ clusters are connected by sharing corners with SiO_4 tetrahedra and form a negatively charged $[(TiO)_4(SiO_4)_3]^{4-}$ framework. The framework has a 3-dimensional system of channels defined by 8-membered rings (8-MRs) with a free (suitable for

migration) crystallographic diameter of ~ 3.5 Å (Yakovenchuk *et al.*, 2009). The channels are occupied by extra-framework cations (*e.g.* Na$^+$, K$^+$, Cu^{2+}) and H$_2$O molecules.
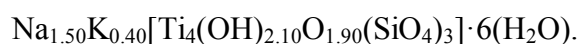
Ivanyukite-Na-T

Ivanyukite-Na-*T* crystallizes in the non-centrosymmetric *R*3*m* space group. In contrast to the cubic compounds (Behrens *et al.*, 1996; Rocha and Anderson, 2000; Xu *et al.*, 2004), the crystal structure contains two crystallographically independent Ti sites (Fig. 4a). Both TiO$_6$ octahedra have very similar average <Ti−O> bond lengths of 1.959 and 1.931 Å, but their polyhedral volumes are somewhat different, 9.77 and 9.36 Å^3 for Ti1O$_6$ and Ti2O$_6$ polyhedra, respectively. The framework contains one independent Si and five independent O sites. The Si−O bond lengths are in the range 1.63-1.68 Å with the mean <Si−O> distance of 1.655 Å. In contrast to the previously reported structure (Yakovenchuk *et al.*, 2009), there is an additional half-populated O8 (H$_2$O) site present located near (1.45 Å) the K1 site. The additional H$_2$O site is likely to be populated when the K1 site is vacant. The geometry of the extra-framework cation configuration is very close to that described by Yakovenchuk *et al.* (2009), with Na atoms in fivefold and K atoms in sevenfold coordination. The K site forms bonds to three framework O sites, two of which are bonded to the Ti2 site of the smaller Ti2O$_6$ octahedron. Dadachov and Harrison (2007) pointed out that the symmetry reduction from cubic to trigonal observed for Na$_4$[(TiO)$_4$(SiO$_4$)$_3$]·6H$_2$O compound occurs as a result of inclusion of an additional guest Na1 cation and its interaction with the framework O atoms. The same is the case for the crystal structure of ivanyukite-Na-*T*, where extra-framework cations are located in the framework cavities (Fig. 5a) and interact with framework O atoms, inducing the rhombohedral distortion. The structural formula of ivanyukite-Na-*T* determined from the structure refinement can be written as Na$_{1.60}$K$_{0.50}$[Ti$_4$O$_{2.10}$(OH)$_{1.90}$(SiO$_4$)$_3$]·5.5(H$_2$O).

Ivanyukite-Na-C

Like the majority of the pharmacosiderite-supergroup minerals (Rumsey *et al.*, 2010), cubic ivanyukite-Na-*C* crystallizes in the $P\bar{4}3m$ space group (Fig. 4b). The framework sites contain one symmetrically independent Si1 and one Ti1 site coordinated by the O1 and O2 atoms. The mean bond lengths for SiO_4 tetrahedra, <1.640> Å, and TiO_6 octahedra, <1.947> Å, are in good agreement with their full occupancies. The K1 site is situated at the center of the 8-MR with the site occupation factor (s.o.f.) = 0.42 and is bonded to eight O2 and four $O3(H_2O)$ atoms with the bond lengths of 3.228(3) and 3.185(4) Å, respectively. The Na atoms occupy the 24*j* site located at 1.51 Å from the K1 site. Due to the short Na1-Na1 distance (~1.5 Å), this site is predominantly vacant with the assigned occupancy $Na_{0.10}H_2O_{0.15}$. The Na atoms are 6-coordinated by two O2, two O3 (H_2O) and two O4 (H_2O) atoms. Such a coordination of Na in pharmacosiderite-type compounds has not been observed previously. In the crystal structure of Na germanate compound (Nowotny and Wittmann, 1954), two Na sites are located at the centers of the 8-MRs (also one site disordered), whereas, in the structure of natropharmacosiderite, Na occupies a splitted site at the center of the 8-MR (Hager *et al.*, 2010). The refined crystal chemical formula of ivanyukite-Na-*C* can be written as $Na_{1.20}K_{0.75}[Ti_4(OH)_{2.05}O_{1.95}(SiO_4)_3]\cdot5.8(H_2O)$.

Refinement of the same material in the *R*3*m* space group yields a model similar to that of ivanyukite-Na-*T*, but with the slightly different extra-framework composition. The O8 site is vacant, but the O6 and O7 H_2O sites are fully populated. The increasing H_2O content is associated with the slight increase in the unit-cell volume from 1408.5(12) (for ivanyukite-Na-*T*) to 1424.2(10) Å^3. Compared to ivanyukite-Na-*T*, the occupancies of the Na1 and K1 sites decrease slightly. The crystal chemical formula can be written as $Na_{1.50}K_{0.40}[Ti_4(OH)_{2.10}O_{1.90}(SiO_4)_3]\cdot6(H_2O)$.

Ivanyukite-K

Ivanyukite-K was obtained through decationization of the crystal of ivanyukite-Na-*T* used for the structure refinement. The crystal structure was solved in the $P\bar{4}3m$ space group (Fig. 4b) and refined to $R_1 = 0.048$. The crystal structure of ivanyukite-K has the same framework as ivanyukite-Na-*C* and contains independent Si and Ti sites and two O sites. The extra-framework content (Fig. 5b) is composed from the fully populated O3 (H_2O) site and the K1 site with s.o.f. $= 0.42$. The refined formula can be written as $K_{1.26}[Ti_4(OH)_{2.74}O_{1.26}(SiO_4)_3]\cdot 4(H_2O)$.

Cu-rich ivanyukite-K

For the initial refinement of the crystal structure of Cu-exchanged ivanyukite, the structure model of ivanyukite-K was used. The K1 site has an occupancy of 0.25. An additional electron-density peak of 4 e^- was observed near the K1 site (1.17 Å) (Fig. 6b) that was interpreted as an additional O3 (H_2O) site with s.o.f. $= 0.5$. Cu was assigned to the O4 site (identical to the O3 site in the crystal structure of ivanyukite-K) with mixed occupancy $(H_2O)_{0.19}Cu_{0.14}$. According to the structure refinement, the Cu atoms are coordinated by three O3 and one O2 sites with the Cu-O distances of 2.46 and 2.62 Å, respectively. The refined formula of Cu-rich ivanyukite-K can be written as $Cu_{0.54}K_{0.75}[Ti_4(OH)_{2.17}O_{1.83}(SiO_4)_3]\cdot 3.76(H_2O)$.

Discussion

Twinning and symmetry of ivanyukite-Na-C

The Raman spectrum of ivanyukite-Na-*C* (Fig. 3) contains bands corresponding to both rhombohedral and cubic ivanyukite-type structures. Since the beam diameter is 2-5 μm, this duality may be related to the regular intergrowths of the two ivanyukite-Na polymorphs or to the presence in the same crystal of domains with different symmetries.

In the course of single-crystal X-ray diffraction experiment, a total of 2205 reflections were collected, of which 940 were indexed in the cubic cell and 669 in the rhombohedral cell; 338 reflections overlapped. During data reduction, it was found that the crystal of ivanyukite-Na-*C* was a two-component twin (with the $R3m$ and $P\overline{4}3m$ symmetries) related by a threefold axis (in both cells) with the twinning matrix (0.6697 0.3264 0.3307 / 0.3427 -0.3281 -0.3287 / 0.3668 0.6858 -0.3155) (~ 2/3 1/3 1/3 / 1/3 -1/3 -1/3 / 1/3 2/3 -1/3). The observed difference in the unit-cell parameters of the trigonal and cubic polymorphs results in the significant splitting of intense reflections at high angles of 2θ. For example, the $\overline{1}00$ and $\overline{1}0\overline{1}$ peaks of the cubic and trigonal unit cells correspond to the same reflection, whereas the $\overline{4}00$ and $\overline{4}0\overline{4}$ peaks are separated from each other (Fig. 7c). It is of interest that the refined crystal chemical formulas for ivanyukite-Na-*T* and ivanyukite-Na-*C* are very close to each other: $(Na_{1.20}K_{0.75}[Ti_4(OH)_{2.05}O_{1.95}(SiO_4)_3]\cdot5.8(H_2O)$ and $Na_{1.50}K_{0.40}[Ti_4(OH)_{2.10}O_{1.90}(SiO_4)_3]\cdot6(H_2O)$, respectively. It is quite probable that this composition is on the border of stability between the two forms. It can be hypothesized that ivanyukite-Na was initially trigonal and transformed into the cubic form after partial loss of Na. The transformation was accompanied by the migration of K^+ cations. The further decrease of the extra-framework Na content through the $Na^+ + O^{2-} \leftrightarrow \square + OH^-$ substitution mechanism (protonation) results in the formation of ivanyukite-K.

Ion-exchange induced transition $R3m \rightarrow P\overline{4}3m$

The transformation of ivanyukite-Na-*T* into cubic form owing to the release of Na in aqueous solutions of NH_4Cl, $CsCl$, $RbCl$, $CuSO_4$, and Clerici solutions was reported previously by Yakovenchuk *et al.* (2008). Additionally, Spiridonova *et al.* (2011) demonstrated the $R3m \rightarrow P\overline{4}3m$ space-group change for the Sr- and Rb-exchanged forms of ivanyukite-Na-*T*. The partial loss of Na in ivanyukite-Na-*T* in our experiments leads to the significant reorganization of the extra-framework cations with K atoms migrating to the centers of 8-MRs (Fig. 5). This migration

leads to the weakening of the interaction with the framework oxygen atoms, leading to the relaxation of the structure and its adoption of a higher (cubic) symmetry. The transformation results in the deformation of the −Ti−O−Ti−O− rhombus and the elongation of the Ti···Ti distance from 3.114 Å in ivanyukite-Na-*T* to 3.279 Å in ivanyukite-K and shrinking along the O−O direction (Fig. 8). The transition was observed *in situ* by means of a polarizing microscope; the release of Na and the increase in symmetry was confirmed by the birefringence disappearing under crossed polars during the course of ion-exchange.

Evolution of chemical composition

The key point in the chemical evolution of the ivanyukite-group minerals is the permanent decrease of the Na content along the series ivanyukite-Na-*T* → ivanyukite-Na-*C* → ivanyukite-K → Cu-rich ivanyukite-K → ivanyukite-Cu. The relationships between the chemical compositions of these minerals are shown in Fig. 9. Both ivanyukite-K and ivanyukite-Cu may form directly from ivanyukite-Na-*T*. The cation-exchange experiments with progressive addition of Cu to natural ivanyukite-K produces a green color indicative decationization process in the series ivanyukite-Na-T to Cu-rich ivanyukite-K and potentially ivanyukite-Cu. The addition of Cu to natural ivanyukite-K produces a light-blue colour (Fig. 9) and the subsequent addition of Cu lead to a formation of ivanyukite-Cu with distinctly green color (Fig. 2d, Fig. 9). The decrease in the total cationic charge excluding hydrogen atoms from 18.44 (ivanyukite-Na-*T*), 17.54 (ivanyukite-Na-*C*) to 16.73 (ivanyukite-K) and 16.92 (Cu-rich ivanyukite-K) indicates the significant role of hydrogen atoms in these substitutions that enter the structure through the protonation of the O framework sites.

The ivanyukite group minerals possess outstanding ion-exchange properties exemplified by several different species/polymorphs appearing in the same physical sample (Fig. 10). Ivanyukite-Na with both $R3m$ and $P\overline{4}3m$ domains loses Na by the substitution $Na^+ + O^{2-} \leftrightarrow \square +$

OH$^-$, leading to the formation of ivanyukite-K. The incorporation of Cu derived from alteration of primary minerals (such as djerfisherite, chalcopyrite or chlorbartonite) leads to the formation of ivanyukite-Cu.

Conclusions

The observed mineralogical and structural relations between ivanyukite-Na-*T*, ivanyukite-Na-*C*, ivanyukite-K and Cu-rich ivanyukite-K have confirmed the existence of the 'ivanyukite-Na-*T* → ivanyukite-Na-*C* → ivanyukite-K → Cu-rich ivanyukite-K → ivanyukite-Cu' transformational series (similar to the 'kazakovite → tisinalite' (Khomyakov *et al.*, 1974), 'zirsinalite → lovozerite' (Khomyakov, 1977), 'parakeldyshite → keldyshite' (Kabanova *et al.*, 2020) series). The evolution is governed by the outstanding ion-exchange properties of the pharmacosiderite-structured microporous titanosilicate framework. Ivanyukite-Na-*T* (*R*3*m*) loses Na by the substitution Na$^+$ + O^{2-} ↔ □ + OH$^-$, which is accompanied by the migration of K atoms, resulting in its transformation into ivanyukite-Na-*C* (*P*$\overline{4}$3*m*). The further loss of Na$^+$ by the same process leads to the formation of ivanyukite-K. The ion-exchange reaction K$^+$ + OH$^-$ ↔ Cu^{2+} + O^{2-} results in the formation of ivanyukite-Cu. The nature of the ivanyukite-Na-*C* crystals with separate *R*3*m* and *P*$\overline{4}$3*m* domains was confirmed by Raman spectroscopy and optical observations.

The experimental results of this study are relevant to the understanding of the post-crystallisation processes in the hyperagpaitic rocks of the Kola alkaline massifs and the genesis of new mineral species, leading to the increased mineralogical diversity in these geochemical environments.

References

Agilent Technologies. (2014) CrysAlis CCD and CrysAlis RED. *Oxford Diffraction Ltd, Yarnton, Oxfordshire*.

Anderson, M.W., Terasaki, O., Ohsuna, T., Malley, P.J.O., Philippou, A., Mackay, S.P., Ferreira, A., Rocha, J. and Lidin, S. (1995) Microporous titanosilicate ETS-10: A structural survey. *Philosophical Magazine B*, **71**, 813–841.

Anson, A., Lin, C.C.H., Kuznicki, S.M. and Sawada, J.A. (2009) Adsorption of carbon dioxide, ethane, and methane on titanosilicate type molecular sieves. *Chemical Engineering Science*, **64**, 3683–3687.

Behrens, E.A. and Clearfield, A. (1997) Titanium silicates, $M_3HTi_4O_4(SiO_4)_3 \cdot 4H_2O$ (M=Na$^+$, K$^+$),with three-dimensional tunnel structures for the selective removal of strontium and cesium from wastewater solutions. *Microporous Materials*, **11**, 65–75.

Behrens, E.A., Poojary, D.M. and Clearfield, A. (1996) Syntheses, Crystal Structures, and Ion-Exchange Properties of Porous Titanosilicates, $HM_3Ti_4O_4(SiO_4)_3 \cdot 4H_2O$ (M = H$^+$, K$^+$, Cs$^+$), Structural Analogues of the Mineral Pharmacosiderite. *Chemistry of Materials*, **8**, 1236–1244.

Behrens, E.A., Sylvester, P. and Clearfield, A. (1998a) Assessment of a Sodium Nonatitanate and Pharmacosiderite-Type Ion Exchangers for Strontium and Cesium Removal from DOE Waste Simulants. *Environmental Science & Technology*, **32**, 101–107.

Behrens, E.A., Poojary, D.M. and Clearfield, A. (1998b) Syntheses, X-ray Powder Structures, and Preliminary Ion-Exchange Properties of Germanium-Substituted Titanosilicate Pharmacosiderites: $HM_3(AO)_4(BO_4)_3 \cdot 4H_2O$ (M = K, Rb, Cs; A = Ti, Ge; B = Si, Ge). *Chemistry of Materials*, **10**, 959–967.

Bosi, F., Hatert, F., Hålenius, U., Pasero, M., Miyawaki, R. and Mills, S.J. (2019) On the application of the IMA−CNMNC dominant-valency rule to complex mineral compositions. *Mineralogical Magazine*, **83**, 627–632.

Britvin, S.N., Gerasimova, L.G., Ivanyuk, G.Y., Kalashnikova, G.O., Krzhizhanovskaya, M.G., Krivovivhev, S. V., Mararitsa, V.F., Nikolaev, A.I., Oginova, O.A., Panteleev, V.N., Khandobin, V.A., Yakovenchuk, V.N. and Yanicheva, N.Y. (2016) Application of titanium-containing sorbents for treating liquid radioactive waste with the subsequent conservation of radionuclides in Synroc-type titanate ceramics. *Theoretical Foundations of Chemical Engineering*, **50**, 598–606.

Celestian, A.J., Powers, M. and Rader, S. (2013) In situ Raman spectroscopic study of transient polyhedral distortions during cesium ion exchange into sitinakite. *American Mineralogist*, **98**, 1153–1161.

Chapman, D.M. and Roe, A.L. (1990) Synthesis, characterization and crystal chemistry of microporous titanium-silicate materials. *Zeolites*, **10**, 730–737.

Chukanov, N. V. and Pekov, I.V. (2005) Heterosilicates with Tetrahedral-Octahedral Frameworks: Mineralogical and Crystal-Chemical Aspects. *Reviews in Mineralogy and Geochemistry*, **57**, 105–143.

Clearfield, A. (2001) Structure and ion exchange properties of tunnel type titanium silicates. *Solid State Sciences*, **3**, 103–112.

Coombs, D.S., Alberti, A., Armbruster, T., Artioli, G., Colella, C., Galli, E., Grice, J.D., Liebau, F., Mandarino, J.A., Minato, H., Nickel, E.H., Passaglia, E., Peacor, D.R., Quartieri, S., Rinaldi, R., Ross, M., Sheppard, R.A., Tillmanns, E. and Vezzalini, G. (1998) Recommended nomenclature for zeolite minerals: report of the subcommittee on zeolites of the International Mineralogical Association, Commission on New Minerals and Mineral Names. *Mineralogical Magazine*, **62**, 533–571.

Dadachov, M.S. and Harrison, W.T.A. (1997) Synthesis and Crystal Structure of $Na_4[(TiO)_4(SiO_4)_3] \cdot 6H_2O$, a Rhombohedrally Distorted Sodium Titanium Silicate Pharmacosiderite Analogue. *Journal of Solid State Chemistry*, **134**, 409–415.

Filippi, M. (2004) Oxidation of the arsenic-rich concentrate at the Přebuz abandoned mine (Erzgebirge Mts., CZ): mineralogical evolution. *Science of The Total Environment*, **322**, 271–282.

Filippi, M., Doušová, B. and Machovič, V. (2007) Mineralogical speciation of arsenic in soils above the Mokrsko-west gold deposit, Czech Republic. *Geoderma*, **139**, 154–170.

Frost, R.L. and Kloprogge, J.T. (2003) Raman spectroscopy of some complex arsenate minerals—implications for soil remediation. *Spectrochimica Acta Part A: Molecular and Biomolecular Spectroscopy*, **59**, 2797–2804.

Gerasimova, L.G., Nikolaev, A.I., Shchukina, E.S., Maslova, M. V., Kalashnikova, G.O., Samburov, G.O. and Ivanyuk, G.Y. (2019) Hydrochloric Acidic Processing of Titanite Ore

to Produce a Synthetic Analogue of Korobitsynite. *Minerals*, **9**, 315.

Hager, S.L., Leverett, P., Williams, P.A., Mills, S.J., Hibbs, D.E., Raudsepp, M., Kampf, A.R. and Birch, W.D. (2010) The single-crystal X-ray structures of bariopharmacosiderite-C, bariopharmacosiderite-Q and natropharmacosiderite. *The Canadian Mineralogist*, **48**, 1477–1485.

Hatert, F. and Burke, E.A.J. (2008) The IMA-CNMNC dominant-constituent rule revisited and extended. *The Canadian Mineralogist*, **46**, 717–728.

Kabanova, N.A., Panikorovskii, T.L., Shilovskikh, V. V., Vlasenko, N.S., Yakovenchuk, V.N., Aksenov, S.M., Bocharov, V.N. and Krivovichev, S. V. (2020) The $Na_{2-n}H_n[Zr(Si_2O_7)]\cdot mH2O$ Minerals and Related Compounds (n = 0–0.5; m = 0.1): Structure Refinement, Framework Topology, and Possible Na^+-Ion Migration Paths. *Crystals*, **10**, 1016.

Khomyakov, A.P. (1977) New data on mineralogy of lovozerite group. *Doklady Akademii Nauk SSSR*, **237**, 199–202.

Khomyakov, A.P., Semenov, E.I., Es'kova, E.M. and Voronkov, A.A. (1974) Kazakovite - a new mineral of the lovozerite group. *Zapiski RMO*, **103**, 342–345.

Krivovichev, S. (2005) Topology of Microporous Structures. *Reviews in Mineralogy and Geochemistry*, **57**, 17–68. Mineralogical Society of America, Chantilly, virginia.

Lafuente, B., Downs, R.T., Yang, H. and Stone, N. (2015) The power of databases: the RRUFF project. Pp. 1–30 in: *Highlights in Mineralogical Crystallography*.

Lin, C.C.H., Dambrowitz, K.A. and Kuznicki, S.M. (2012) Evolving applications of zeolite molecular sieves. *The Canadian Journal of Chemical Engineering*, **90**, 207–216.

Majzlan, J., Haase, P., Plášil, J. and Dachs, E. (2019) Synthesis and stability of some members of the pharmacosiderite group, $AFe_4(OH)_4(AsO_4)_3\cdot nH_2O$ (A = K, Na, 0.5Ba, 0.5Sr). *The Canadian Mineralogist*, **57**, 663–675.

Milne, N.A., Griffith, C.S., Hanna, J. V., Skyllas-Kazacos, M. and Luca, V. (2006) Lithium Intercalation into the Titanosilicate Sitinakite. *Chemistry of Materials*, **18**, 3192–3202.

Momma, K. and Izumi, F. (2011) VESTA 3 for three-dimensional visualization of crystal, volumetric and morphology data. *Journal of Applied Crystallography*, **44**, 1272–1276.

Nickel, E.H. and Grice, J.D. (1998) The IMA Commission on New Minerals and Mineral Names: procedures and guidelines on mineral nomenclature, 1998. *Mineralogy and Petrology*, **64**, 237–263.

Nowotny, H. and Wittmann, A. (1954) Zeolithische Alkaligermanate. *Monatshefte für Chemie*, **85**, 558–574.

Oleksiienko, O., Wolkersdorfer, C. and Sillanpää, M. (2017) Titanosilicates in cation adsorption

and cation exchange – A review. *Chemical Engineering Journal*, **317**, 570–585.

Pakhomovsky, Y.A., Panikorovskii, T.L., Yakovenchuk, V.N., Ivanyuk, G.Y., Mikhailova, J.A., Krivovichev, S. V., Bocharov, V.N. and Kalashnikov, A.O. (2018) Selivanovaite, $NaTi_3(Ti,Na,Fe,Mn)_4[(Si_2O_7)_2O_4(OH,H_2O)_4]\cdot nH_2O$, a new rock-forming mineral from the eudialyte-rich malignite of the Lovozero alkaline massif (Kola Peninsula, Russia). *European Journal of Mineralogy*, **30**, 525–535.

Popa, K. and Pavel, C.C. (2012) Radioactive wastewaters purification using titanosilicates materials: State of the art and perspectives. *Desalination*, **293**, 78–86.

Rocha, J. and Anderson, M.W. (2000) Microporous Titanosilicates and other Novel Mixed Octahedral-Tetrahedral Framework Oxides. *European Journal of Inorganic Chemistry*, **2000**, 801–818.

Rumsey, M.S., Mills, S.J. and Spratt, J. (2010) Natropharmacoalumite, $NaAl_4[(OH)_4(AsO_4)_3]\cdot 4H_2O$, a new mineral of the pharmacosiderite supergroup and the renaming of aluminopharmacosiderite to pharmacoalumite. *Mineralogical Magazine*, **74**, 929–936.

Seki, T., Chiang, K.-Y., Yu, C.-C., Yu, X., Okuno, M., Hunger, J., Nagata, Y. and Bonn, M. (2020) The Bending Mode of Water: A Powerful Probe for Hydrogen Bond Structure of Aqueous Systems. *The Journal of Physical Chemistry Letters*, **11**, 8459–8469.

Sheldrick, G.M. (2015) Crystal structure refinement with SHELXL. *Acta Crystallographica Section C Structural Chemistry*, **71**, 3–8.

Spiridonova, D. V., Krivovichev, S. V., Yakovenchuk, V.N. and Pakhomovsky, Y.A. (2011) Crystal structures of the Rb- and Sr-exchanged forms of ivanyukite-Na-T. *Geology of Ore Deposits*, **53**, 670–677.

Xu, H., Navrotsky, A., Nyman, M. and Nenoff, T.M. (2004) Crystal chemistry and energetics of pharmacosiderite-related microporous phases in the $K_2O–Cs_2O–SiO_2–TiO_2–H_2O$ system. *Microporous and Mesoporous Materials*, **72**, 209–218.

Yakovenchuk, V., Pakhomovsky, Y., Panikorovskii, T., Zolotarev, A., Mikhailova, J., Bocharov, V., Krivovichev, S. and Ivanyuk, G. (2019) Chirvinskyite, $(Na,Ca)_{13}(Fe,Mn,\square)_2(Ti,Nb)_2(Zr,Ti)_3(Si_2O_7)_4(OH,O,F)_{12}$, a New Mineral with a Modular Wallpaper Structure, from the Khibiny Alkaline Massif (Kola Peninsula, Russia). *Minerals*, **9**, 219.

Yakovenchuk, V.N., Selivanova, E.A., Ivanyuk, G.Y., Pakhomovsky, Y.A., Spiridonova, D. V. and Krivovichev, S. V. (2008) First Natural Pharmacosiderite-Related Titanosilicates and Their Ion-Exchange Properties. Pp. 27–35 in: *Minerals as Advanced Materials I*. Springer Berlin Heidelberg, Berlin, Heidelberg.

Yakovenchuk, V.N., Nikolaev, A.P., Selivanova, E.A., Pakhomovsky, Y.A., Korchak, J.A., Spiridonova, D. V., Zalkind, O.A. and Krivovichev, S. V. (2009) Ivanyukite-Na-T, ivanyukite-Na-C, ivanyukite-K, and ivanyukite-Cu: New microporous titanosilicates from the Khibiny massif (Kola Peninsula, Russia) and crystal structure of ivanyukite-Na-T. *American Mineralogist*, **94**, 1450–1458.

Yakovenchuk, V.N., Selivanova, E.A., Krivovichev, S. V., Pakhomovsky, Y.A., Spiridonova, D. V., Kasikov, A.G. and Ivanyuk, G.Y. (2011) Ivanyukite-Group Minerals: Crystal Structure and Cation-Exchange Properties. Pp. 205–211 in: *Minerals as Advanced Materials II.* Springer Berlin Heidelberg, Berlin, Heidelberg.

Table 1. Chemical composition of ivanyukite group minerals

Source	This work	This work	Yakovenchuk *et al.* 2009**	This work	Yakovenchuk *et al.* 2009**	This work
sample	Ivanyukite-Na-*T* MEC-3184	Ivanyukite-Na-C MEC-3184	Ivanyukite-K	Ivanyukite-K exchanged-form	Ivanyukite-Cu	Cu-rich ivanyukite-K exchanged-form
SiO_2	25.19	25.40	23.16	27.20	24.80	27.19
TiO_2	40.86	40.29	36.14	43.76	38.36	42.89
Al_2O_3	0.07	0.14	0.18	0.08	0.07	0.08
FeO	0.30	0.20	0.37	0.33	0.73	0.33
MnO	0.03	0.10	0.68	0.11	0.28	0.05
CaO	0.24	0.16	0.95	0.34	0.23	0.34
Na_2O	7.93	5.63	0.27	0.56	0.17	0.02
K_2O	6.06	6.44	7.09	7.61	2.80	5.40
H_2O*	15.81	17.84	25.00	15.32	21.50	14.40
CuO	n/d	n/d	2.21	n/d	6.81	5.40
Nb_2O_5	3.34	3.00	3.62	3.41	3.02	3.40
Total	99.83	99.20	99.67	98.72	99.67	99.50
Atoms per formula unit normalized on the basis of 3 Si atoms						
Si^{4+}	3.00	3.00	3.00	3.00	3.00	3.00
Ti^{4+}	3.66	3.58	3.52	3.63	3.49	3.56
Al^{3+}	0.01	0.02	0.03	0.01	0.01	0.01
Fe^{2+}	0.03	0.02	0.04	0.03	0.07	0.03
Mn^{2+}	0.00	0.01	0.07	0.01	0.03	0.00
Nb^{5+}	0.18	0.16	0.21	0.17	0.17	0.17
Sum *O*	3.88	3.79	3.87	3.84	3.77	3.77
Ca^{2+}	0.03	0.02	0.13	0.04	0.03	0.04
Na^+	1.83	1.29	0.07	0.12	0.04	0.00
K^+	0.92	0.97	1.17	1.07	0.43	0.76
Cu^{2+}	n/d	n/d	0.22	n/d	0.62	0.45
Sum *A*	2.78	2.28	1.59	1.23	1.12	1.25
OH^-	12.56	14.06	21.60	11.27	17.35	10.60

*Content of H_2O calculated according to structural data for investigated samples in this work.

**For literature data in ivanyukite-K detected 0.19 wt.% SrO and 0.20 wt.% SO_3 for

Ivanyukite-Cu

n/d – not detected

Table 2. Raman shifts in the ivanyukite group minerals spectra and their assignment

Raman shift, cm^{-1}			Assignment
ivanyukite-Na-*T* MEC-3184	ivanyukite-Na-*C* MEC-3183	Cu-rich ivanyukite-K exchanged-form	
126	128		*lattice vibrations*
217	219	229	TiO$_6$
258s	255s	266	TiO$_6$
323	319		TiO$_6$
		342	TiO$_6$
355	356		SiO$_4$
370	378		SiO$_4$
	460	493	TiO$_6$
		533s	SiO$_4$, TiO$_6$
586s	595s	599	SiO$_4$, TiO$_6$
	714	716w	OH
844	845	840	SiO$_4$
934s	929s	961s	SiO$_4$
	1030w		SiO$_4$
1624	1625	1605	H$_2$O
3250	3250		OH
		3310w	OH
		3350	OH
	3388		OH
3450	3440	3440	H$_2$O

sh = shoulder. s = strong intensity. w = weak

Table 3. Data collection information and structure-refinement parameters for ivanyukite group of minerals

Mineral	ivanyukite-Na-T	ivanyukite-Na-C	ivanyukite-Na-C	ivanyukite-K	Cu-rich ivanyukite-K
Temperature/K	293(2)	293(2)	293(2)	293(2)	293(2)
Crystal system	trigonal	cubic	trigonal	cubic	cubic
Space group	R3m	P-43m	R3m	P-43m	P-43m
$a=b$ /Å	10.932(4)	7.784(2)	10.926(3)	7.8711(3)	7.8507(6)
c/Å	13.609(7)	7.784(2)	13.776(4)	7.8711(3)	7.8507(6)
γ/°	120	90	120	90	90
Volume/Å^3	1408.5(12)	471.6(3)	1424.2(10)	487.65(6)	483.87(11)
Z	3	1	3	1	1
ρ_{calc}g/cm^3	2.420	2.407	2.343	2.197	2.298
μ/mm^{-1}	2.085	2.127	2.028	2.121	2.839
Crystal size/mm^3	0.11 × 0.11 × 0.02	0.17 × 0.17 × 0.17	0.17 × 0.17 × 0.17	0.11 × 0.11 × 0.02	0.07× 0.07 × 0.02
2Θ range for data collection/°	7.376 to 52.926	7.404 to 62.47	7.318 to 52.946	7.322 to 54.828	7.34 to 54.982
Index ranges	-8 ≤ h ≤ 13, -12 ≤ k ≤ 10, -11 ≤ l ≤ 16	-10 ≤ h ≤ 11, -9 ≤ k ≤ 10, -9 ≤ l ≤ 10	-13 ≤ h ≤ 13, -13 ≤ k ≤ 13, -15 ≤ l ≤ 17	-9 ≤ h ≤ 2, -8 ≤ k ≤ 6, -4 ≤ l ≤ 10	-7 ≤ h ≤ 7, -4 ≤ k ≤ 10, -9 ≤ l ≤ 1
Reflections collected	1303	1954	1558	632	648
Independent reflections	531 [R_{int} = 0.0950, R_{sigma} = 0.0700]	318 [R_{int} = 0.1648, R_{sigma} = 0.0919]	711 [R_{int} = 0.0847, R$_{sigma}$ = 0.0886]	243 [R_{int} = 0.0317, R_{sigma} = 0.0311]	246 [R$_{int}$ = 0.0351, R$_{sigma}$ = 0.0329]
Data/restraints/parameters	531/50/72	318/0/26	711/1/69	243/6/21	246/0/24
Goodness-of-fit on F^2	1.137	1.141	1.079	1.247	1.226
Final R indexes [I>=2σ (I)]	R_1 = 0.0997, wR_2 = 0.2515	R_1 = 0.0981, wR_2 = 0.2567	R_1 = 0.0983, wR_2 = 0.2511	R_1 = 0.0482, wR_2 = 0.1200	R_1 = 0.0477, wR_2 = 0.1084

Final R indexes [all data]	$R_1 = 0.1048$, w$R_2 = 0.2583$	$R_1 = 0.1107$, w$R_2 = 0.2670$	$R_1 = 0.1040$, w$R_2 = 0.2588$	$R_1 = 0.0571$, w$R_2 = 0.1298$	$R_1 = 0.0574$, w$R_2 = 0.1172$
Largest diff. peak/hole / e Å^{-3}	1.55/-1.61	1.37/-0.77	1.49/-1.42	0.77/-0.52	0.61/-0.43
Flack parameter	0.45(16)	0.47(14)	0.33(12)	-0.07(5)	0.46(6)

Table 4. Atomic coordinates, displacement parameters (Å^2), and site occupation factors (SOF) for ivanyukite-Na-*T*

Site	occupancy	x/a	y/b	z/c	Uiso
Ti1	Ti	0.1421(4)	0.5710(2)	0.0461(4)	0.0178(12)
Ti2	Ti	0	0	0.1933(6)	0.020(2)
Si1	Si	0.1676(3)	0.3351(6)	0.1686(6)	0.0202(18)
K1	$K_{0.50}$	1/3	2/3	0.323(4)	0.092(19)
Na1	$Na_{0.52}$	0.5313(17)	0.4687(17)	0.230(2)	0.061(8)
O1	O	0.1545(18)	0.0772(9)	0.2931(18)	0.020(4)
O2	O	0.0856(10)	0.171(2)	0.1260(19)	0.028(5)
O3	O	0.1680(9)	0.3359(18)	0.2917(15)	0.019(4)
O4	O	0.0815(13)	0.4123(13)	0.1288(10)	0.019(3)
O5	O	1/3	2/3	0.121(2)	0.0080(17)
O6	$(H_2O)_{0.50}$	0.428(4)	0.2139(18)	0.250(4)	0.093(14)
O7	$(H_2O)_{0.66}$	0.4764(19)	0.5236(19)	0.357(3)	0.053(9)
O8	$(H_2O)_{0.50}$	1/3	2/3	0.429(6)	0.035(9)

Table 5. Atomic coordinates, displacement parameters ($\mathring{A}^2$), and site occupation factors (SOF) for cubic ivanyukite-Na-*C*

Site	Occupancy	x/a	y/b	z/c	Uiso
Ti1	Ti	0.6430(3)	0.3570(3)	0.6430(3)	0.0215(12)
Si1	Si	½	0	½	0.0225(18)
K1	$K_{0.25}$	½	0	0	0.11(3)
Na1	$(H_2O)_{0.15}Na_{0.10}$	0.668(7)	0.070(4)	0.930(4)	0.051(13)
O1	O	0.3845(17)	0.3845(17)	0.6155(17)	0.026(4)
O2	O	0.6224(11)	0.1200(14)	0.6224(11)	0.024(3)
O3	H_2O	0.182(4)	0.182(4)	0.818(4)	0.120(18)

Table 6. Atomic coordinates, displacement parameters (Å^2), and site occupation factors (SOF) for trigonal ivanyukite-Na-*C*

Site	Occupancy	x/a	y/b	z/c	Uiso
Ti1	Ti	0.1418(4)	0.5709(2)	0.0449(3)	0.0182(12)
Ti2	Ti	0	0	0.1967(5)	0.0169(16)
Si1	Si	0.1677(3)	0.3354(7)	0.1689(6)	0.0211(16)
K1	K$_{0.40}$	1/3	2/3	0.316(2)	0.052(13)
Na1	Na$_{0.50}$	0.5329(15)	0.4671(15)	0.2279(16)	0.018(10)
O1	O	0.1531(18)	0.0766(9)	0.2965(15)	0.024(4)
O2	O	0.0848(11)	0.170(2)	0.1288(14)	0.024(5)
O3	O	0.1689(10)	0.338(2)	0.2895(14)	0.026(5)
O4	O	0.0830(15)	0.4131(15)	0.1274(8)	0.022(3)
O5	O	1/3	2/3	0.115(2)	0.019(7)
O6	H$_2$O	0.443(3)	0.2217(14)	0.261(2)	0.054(7)
O7	H$_2$O	0.4798(18)	0.5202(18)	0.355(3)	0.093(16)

Table 7. Atomic coordinates, displacement parameters (Å^2), and site occupation factors (SOF) for ivanyukite-K

Site	Occupancy	x/a	y/b	z/c	Uiso
Ti1	Ti	0.64727(19)	0.35273(19)	0.35273(19)	0.0124(7)
Si1	Si	½	½	0	0.0153(11)
K1	K$_{0.42}$	½	0	0	0.28(4)
O1	O	0.3854(9)	0.3854(9)	0.3854(9)	0.019(3)
O2	O	0.6198(6)	0.3802(6)	0.1190(8)	0.0133(14)
O3	H$_2$O	0.190(2)	0.190(2)	0.190(2)	0.121(10)

Table 8. Atomic coordinates, displacement parameters ($Å^2$), and site occupation factors (SOF) for Cu-rich ivanyukite-K

Site	Occupancy	x/a	y/b	z/c	Uiso
Ti1	Ti	0.3528(2)	0.3528(2)	0.3528(2)	0.0120(7)
Si1	Si	½	0	½	0.0159(12)
Cu1	$Cu_{0.14}(H_2O)_{0.19}$	0.810(2)	0.190(2)	0.190(2)	0.136(13)
K1	$K_{0.25}$	½	0	0	0.09(2)
O1	O	0.6160(10)	0.3840(10)	0.3840(10)	0.016(3)
O2	O	0.3801(6)	0.1196(9)	0.3801(6)	0.0148(16)
O3	$(H_2O)_{0.50}$	0.351(7)	0	0	0.12(2)

Fig. 1. The Koashva career, Khibiny alkaline massif, Kola Peninsula, Russia. The red star indicates the holotype location for the ivanyukite group minerals. Photo by Gregory Ivanyuk.
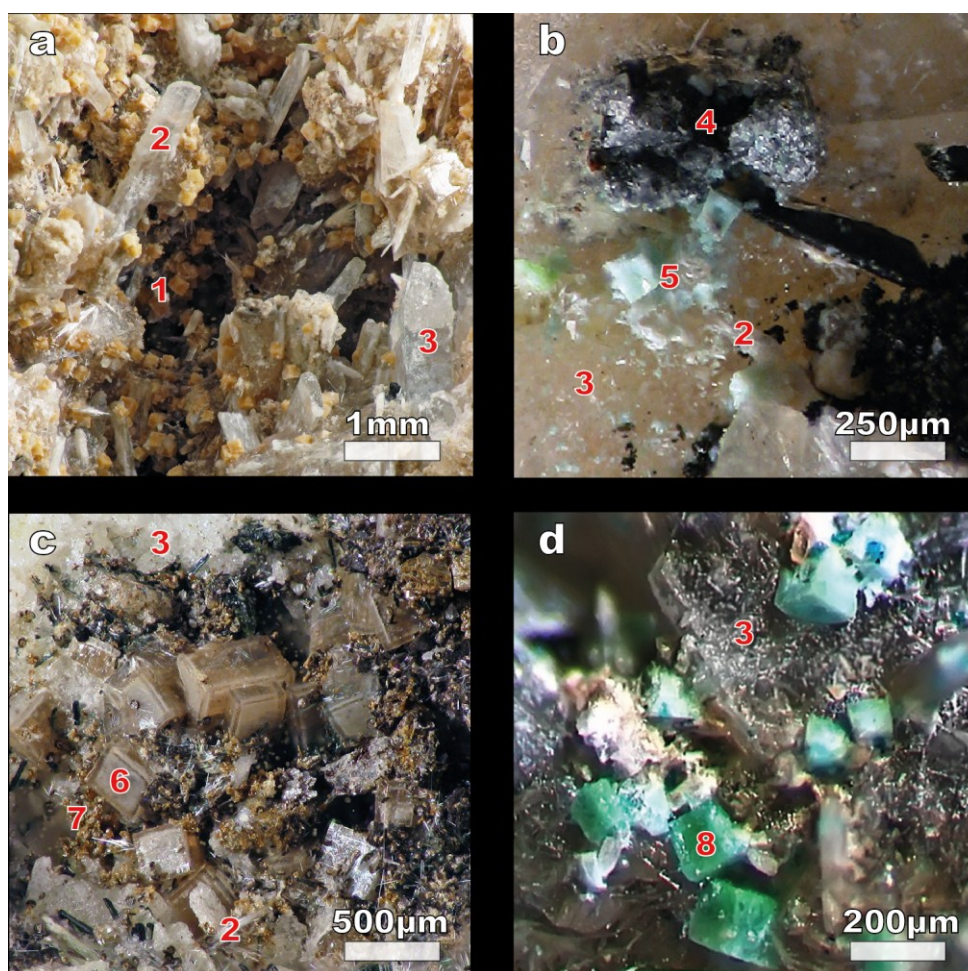
Fig. 2. Photo of ivanyukite group samples: MEC-3183, orange crystals of ivanyukite-Na-*C* (1) with vinogradovite (2) and natrolite (3) (a); crystals of chlorbartonite (4) with light blue ivanyukite-K (5) (b); MEC-3184 ivanyukite-Na-*T* (6) epitactic crusts growing on sitinakite crystals (not marked) with lucasite-(Ce) (7) (c); and ivanyukite-Cu (8) found in the cavity with altered djerfisherite (d). Photo by Gregory Ivanyuk.
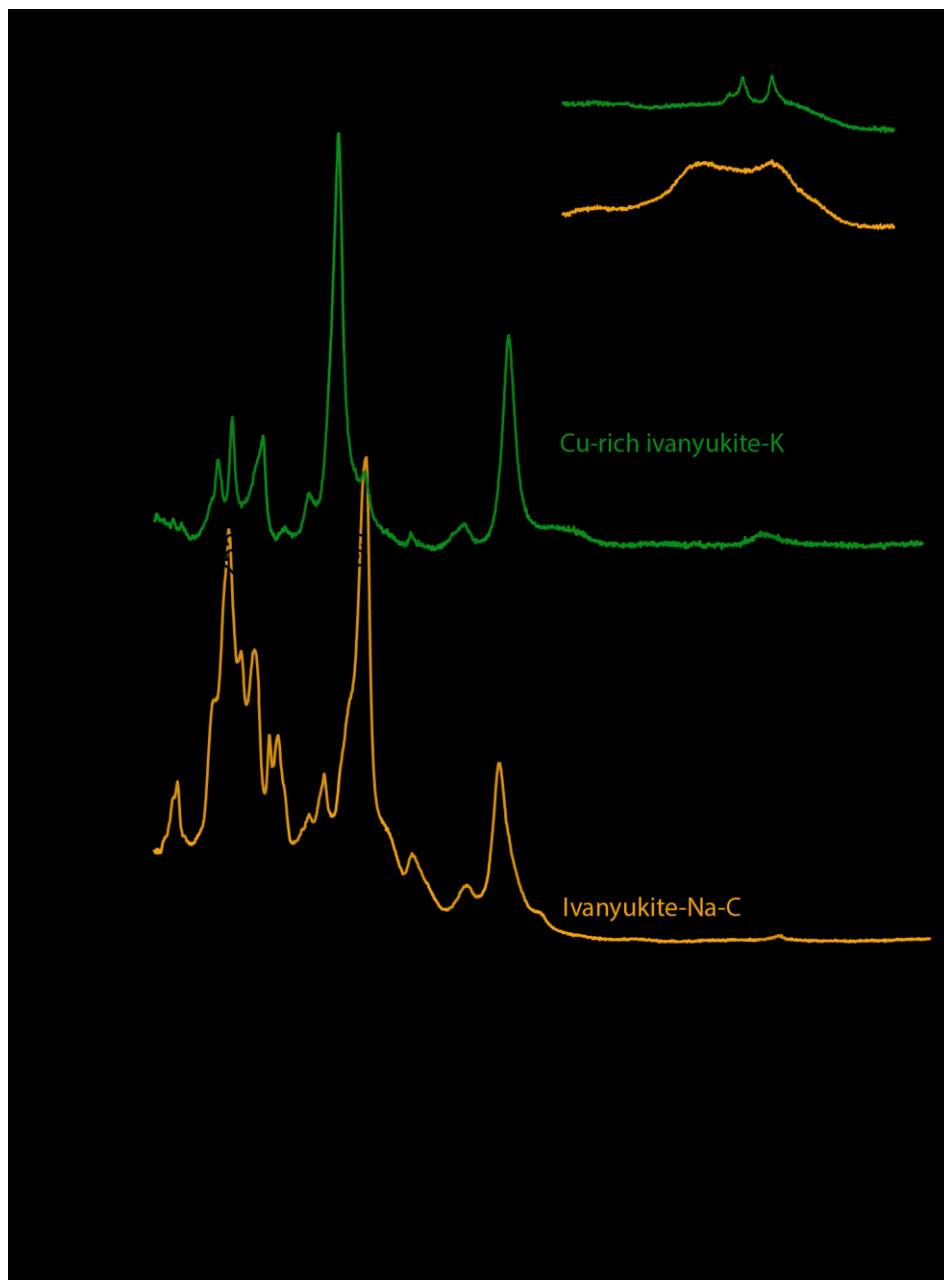
Fig. 3. Raman spectrum of ivanyukite group minerals.
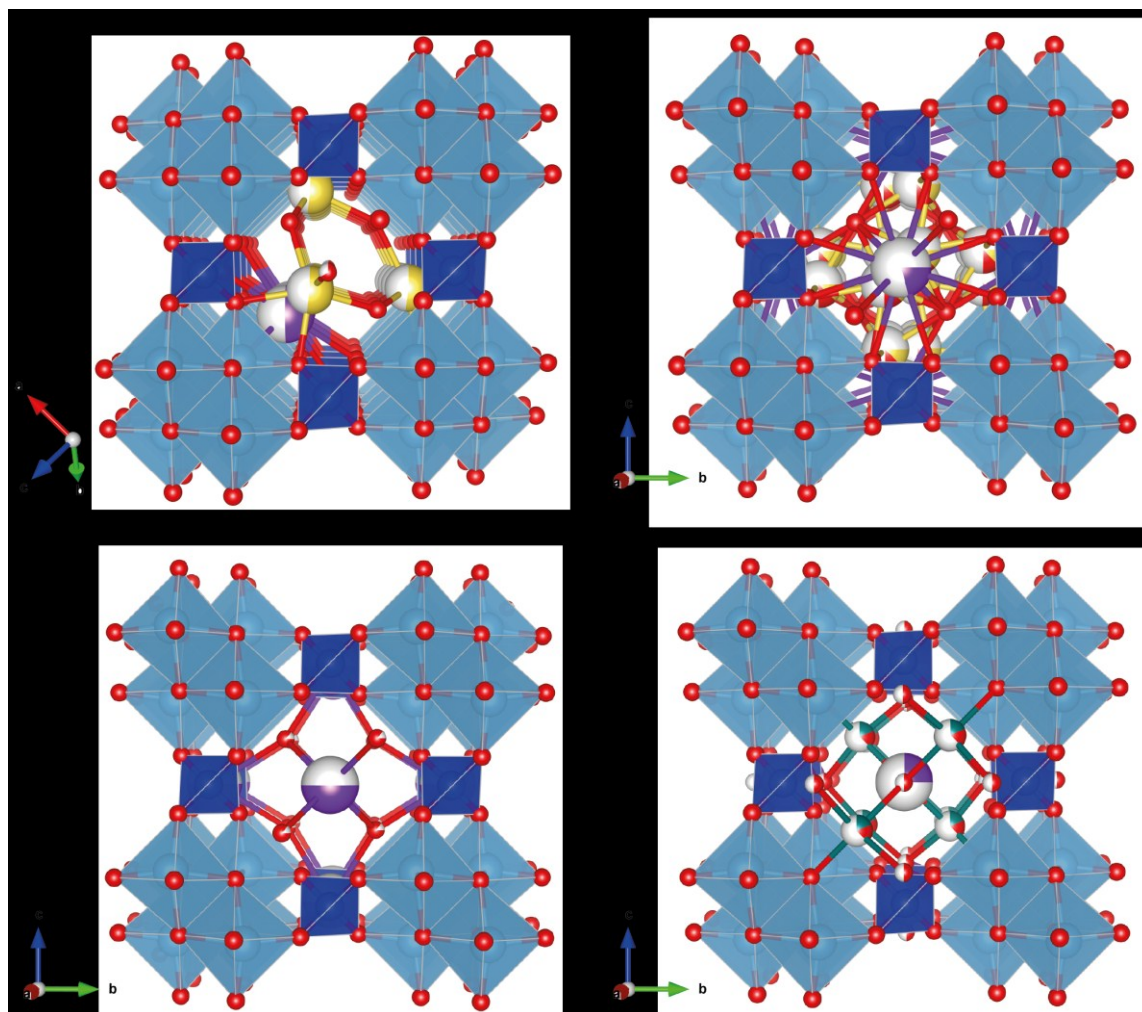
Fig. 4. A general view of crystal structures of ivanyukite group minerals: ivanyukite-Na-*T* (a); ivanyukite-Na-*C* (b); ivanyukite-K (c), Cu-rich ivanyukite-K (d) in cation-centered polyhedral representation (TiO$_6$ octahedra are light blue, SiO$_4$ tetrahedra are blue, oxygen sites shown as red spheres, K – lilac, Na – yellow, Cu - teal. The spheres filled according to atom occupancy.
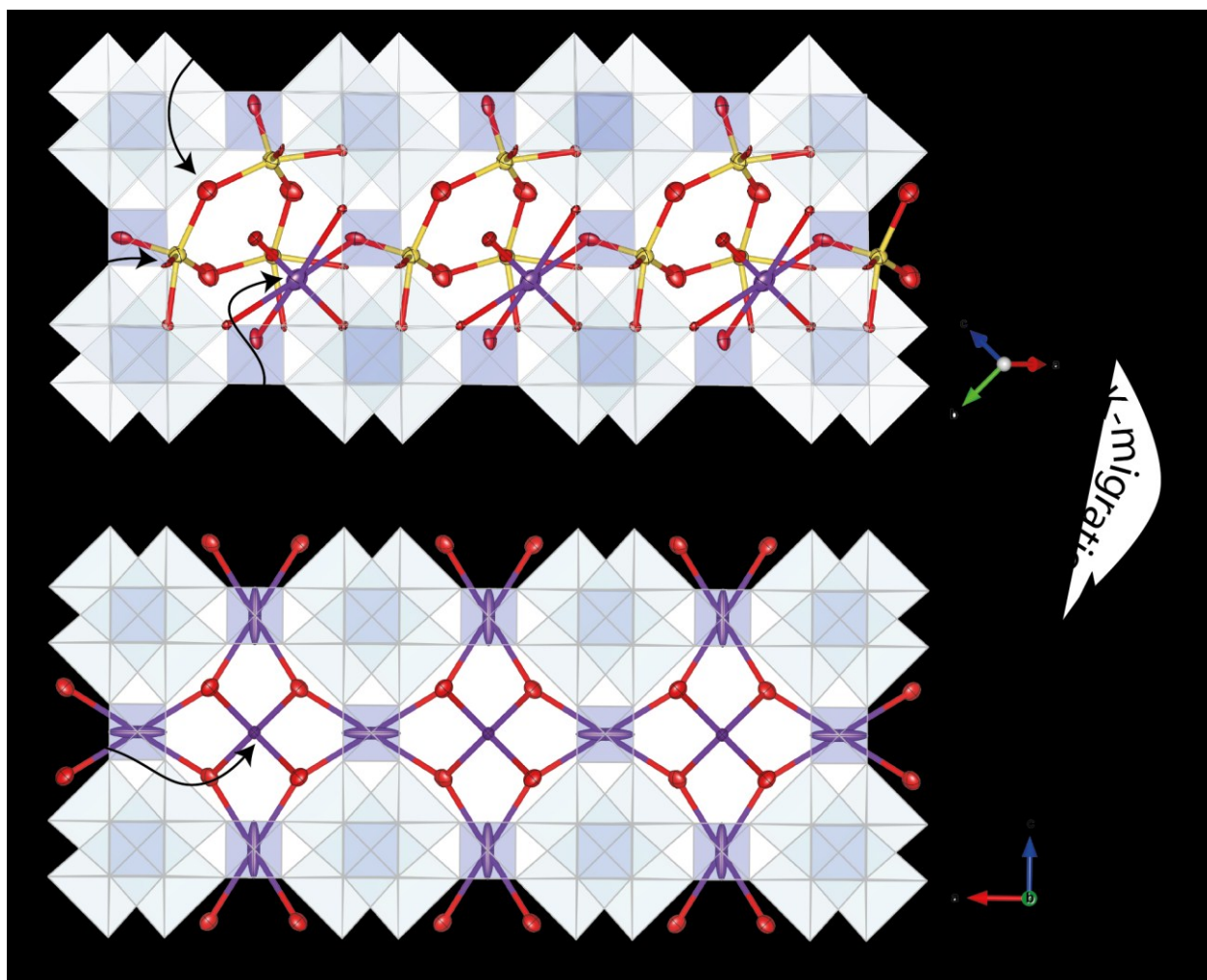
Fig. 5. Arrangement of extra-framework cations in the crystals structures of ivanyukite-Na-*T* (a) and in in the crystal structure ivanyukite-K (b).
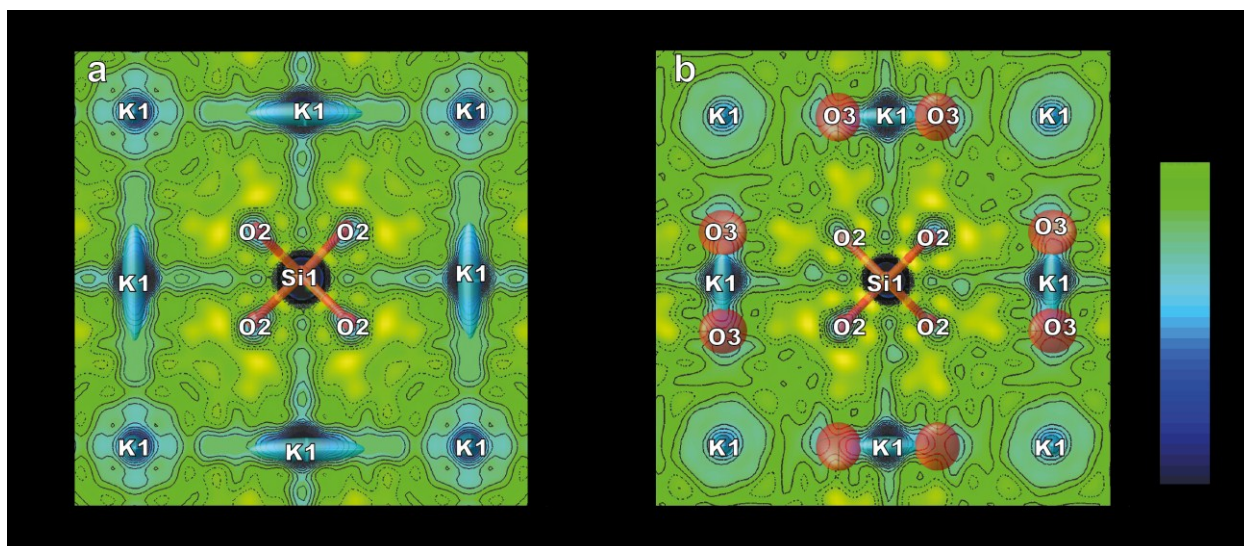
Fig. 6. Observed electron density map around K1 and O3 sites (projection on (001) plane), contour intervals are 0.5 eÅ^{-3} in the crystal structures of ivanyukite-K (a), Cu-rich ivanyukite-K (b).
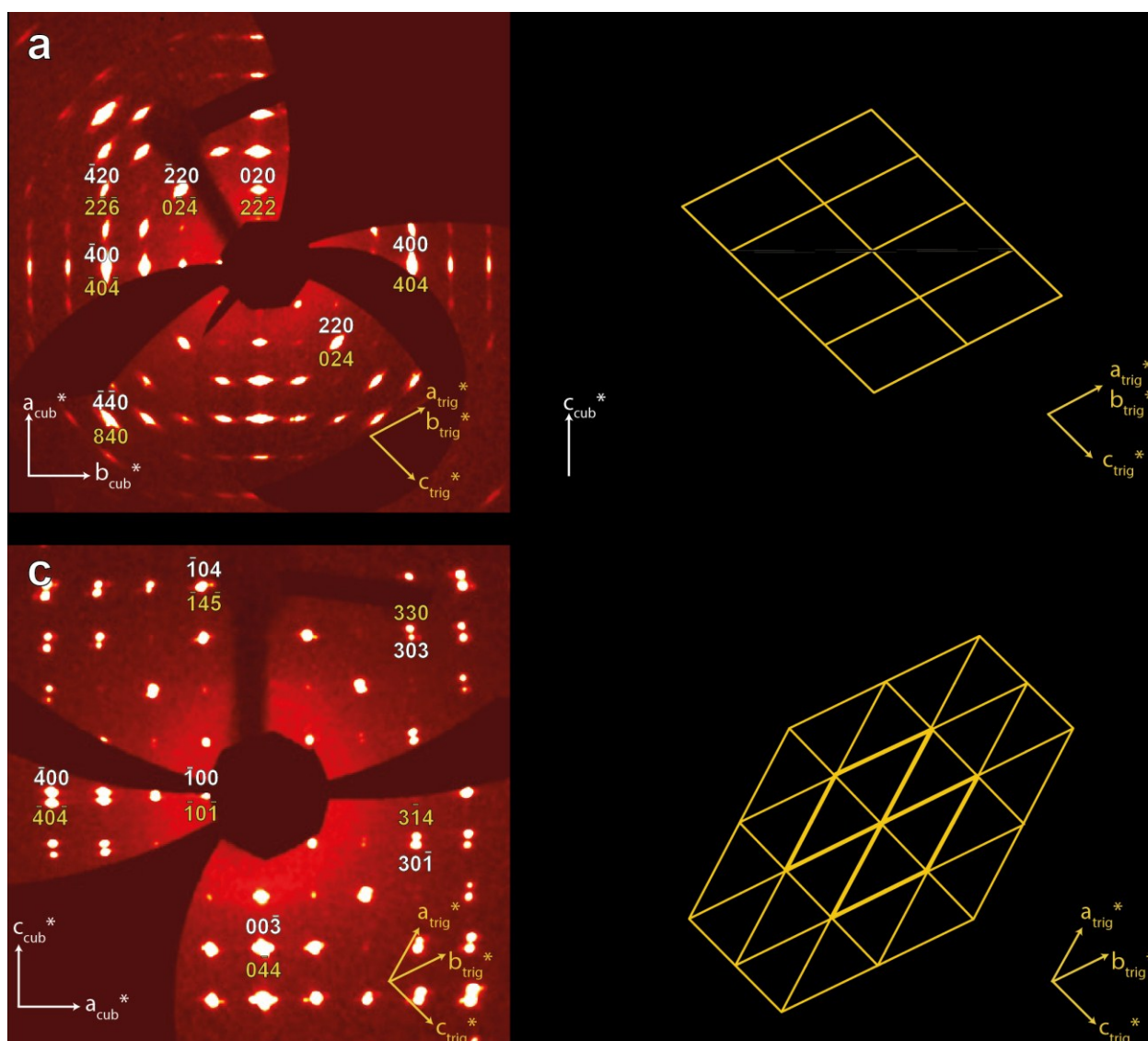
Fig. 7. Reconstructed *hk*0 section of reciprocal space obtained from the ivanyukite-Na-*C* crystal studied (a), Generation of a reciprocal lattices with cubic (black) and trigonal (orange) symmetry oriented on the *hk*0 section of reciprocal space (b), *h*0*l* section of reciprocal space (c), reciprocal lattices oriented on the *h*0*l* section of reciprocal space (d).
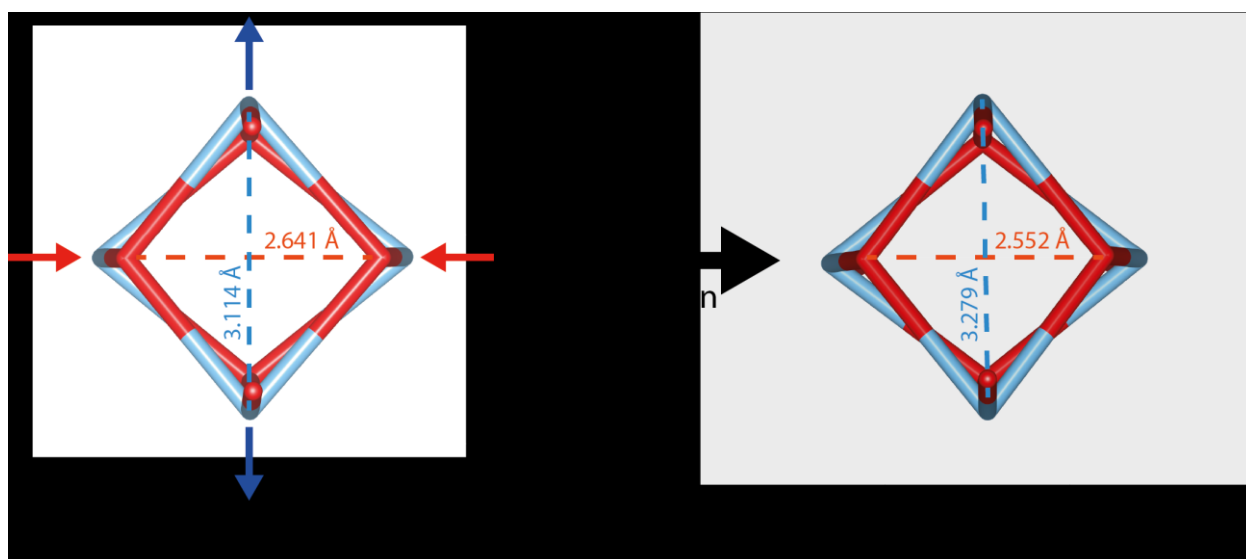
Fig. 8. Distortion of a cubane-like cluster in the rhombohedral structure of ivanyukite-Na-*T* in comparison to its ideal cubic symmetry in the crystal structure ivanyukite-K.
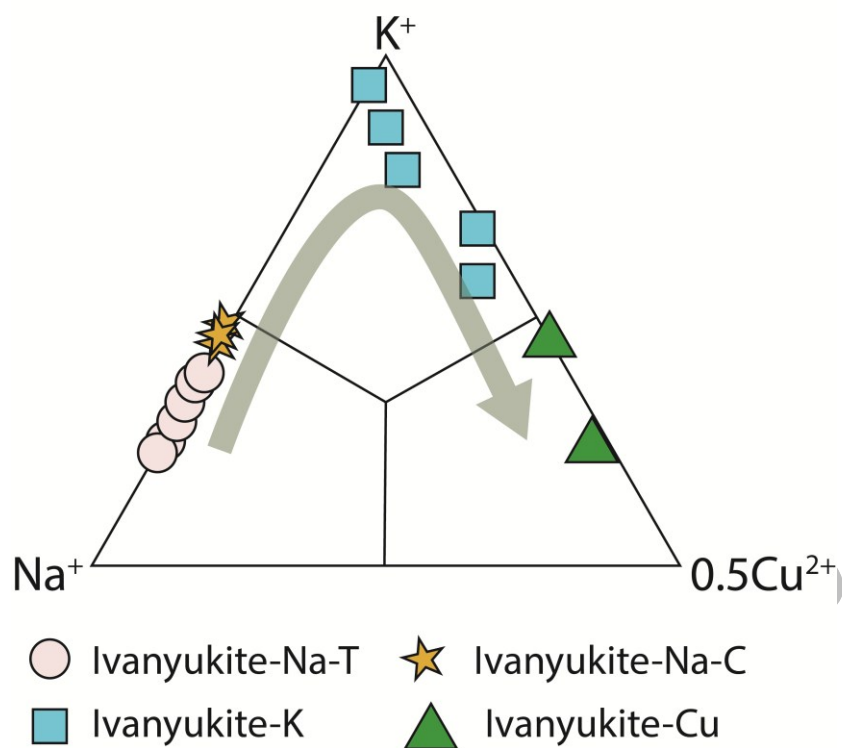
Fig. 9. Relation between content of main extra-framework cations K, Na and Cu in the ivanyukite group minerals after (Yakovenchuk et al. 2009) with our data plotted. Green arrow indicates evolution of chemical composition through time.
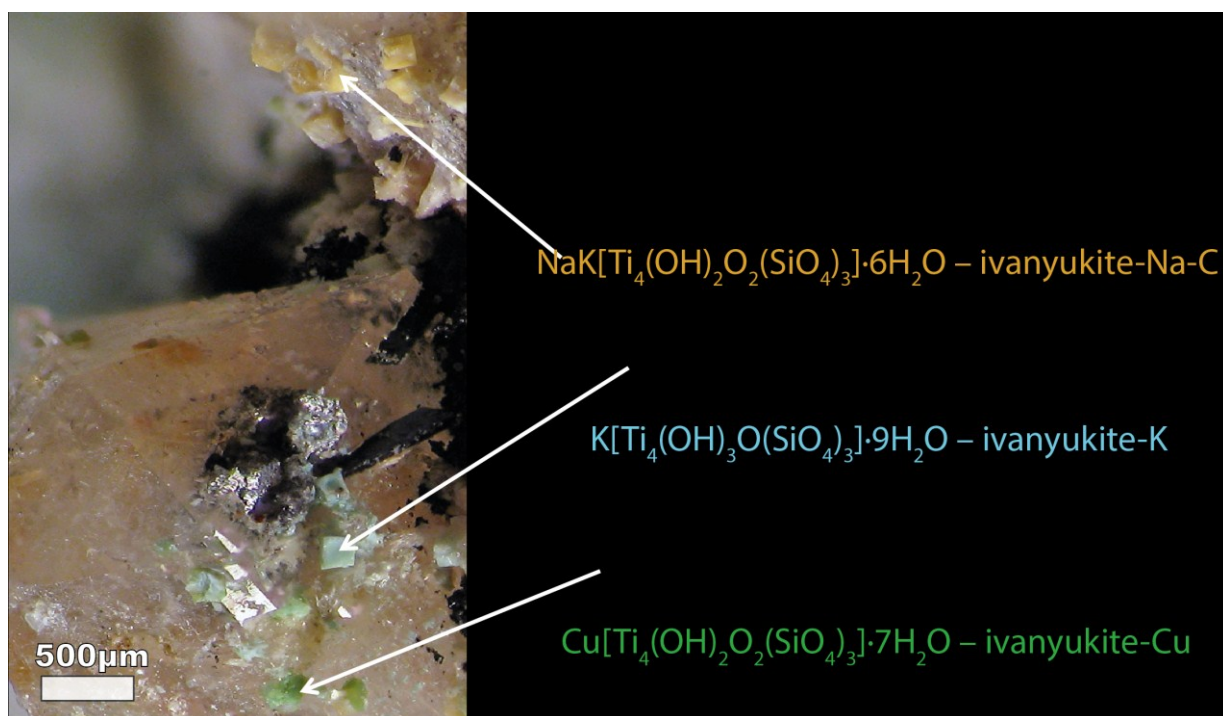
Fig. 10. Evolution of ivanyukite group minerals: free species in one sample, Koashva mine, Khibiny. The sample from private collection VNY (under study).